Mixing and decoherence in continuous-time quantum walks on long-range interacting cycles

Mixing and decoherence in continuous-time quantum walks on long-range interacting cycles

S Salimi and R Radgohar

Faculty of Science, Department of Physics, University of Kurdistan, Pasdaran Ave., Sanandaj, Iran

E-mail: shsalimi@uok.ac.ir and r.radgohar@uok.ac.ir

Abstract
We study the effect of small decoherence in continuous-time quantum walks on long-range interacting cycles, which are constructed by connecting all the two nodes of distance m on the cycle graph. In our investigation, each node is continuously monitored by an individual point contact, which induces the decoherence process. We obtain the analytical probability distribution and the mixing time upper bound. Our results show that, for small rates of decoherence, the mixing time upper bound is independent of distance parameter m and is proportional to inverse of decoherence rate.

PACS numbers: 03.65.Yz, 03.67.−a

1. Introduction

Random walks on graphs have broad applications in various fields of mathematics, computer science and natural sciences, such as mathematical modeling of physical systems and simulated annealing [1]. The quantum mechanical analog of the random walks on complex networks has been studied with respect to the localization and delocalization transition in the presence of site disorder [2–4]. Quantum walks (QWs) have been largely divided into two standard variants, the discrete-time QWs (DTQWs) [5, 6] and the continuous-time QWs (CTQWs) [7]. The DTQWs have been investigated on trees [8], on random environments [9], for single and entangled particles [10] and also in [1, 11, 12]. In the recent years, the CTQWs have been studied on the n-cube [13], star graph [14, 15], small-world network [16], quotient graph [17], line [18–20], dendrimer [21], distance regular graph [22], circulant Bunkbeds [23], odd graph [24] and decision tree [25, 26].

In all of these cited works it has been supposed that we have a closed quantum system without any interaction with its environment. Firstly, Kendon and Tregenna considered the effect of decoherence in quantum walks in 'Decoherence can be useful in quantum walks' [27]. By numerical observation, they found that a small amount of decoherence can be useful to
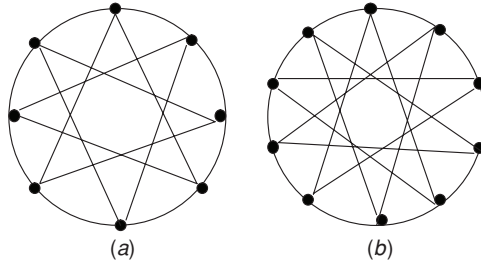
Figure 1. Long-range interaction cycles $G(8; 3)$ and $G(10; 4)$

decrease the mixing time of discrete quantum walks on cycles. Then decoherence in quantum walks has been studied on line [28], on circulant [29] and on hypercube [29]. In 'Mixing and decoherence in continuous-time quantum walks on cycles' [30], an analytical counterpart to Kendon and Tregenna's result for the continuous-time quantum walk on cycles has been provided. Its results show that, for small rates of decoherense, the mixing time decreases linearly with decoherence while for large rates of decoherence, the mixing time increases linearly toward the classical limit. Moreover, for the middle region of decoherence rates, the numerical data confirm the existence of a unique optimal rate in which the mixing time is minimal.

In this paper, we consider the effect of decoherence in continuous-time quantum walks on long-range interacting cycles (LRICs) as the extensions of the cycle graphs. LRICs are constructed by connecting all the two nodes of distance m on the cycle graph (nearest-neighboring lattice). A detailed description of the network structure will be given in the next section. Numerical analysis of CTQWs on LRICs has been provided in 'Coherent exciton transport and trapping on long-range interacting cycles' [3]. We take a small amount of decoherence into account and by analytical technique show it can decrease the mixing time in continuous-time quantum walks on LRICs.

For this end, we use the Gurvitz model [31]. In this model, each vertex is monitored by a corresponding point contact induced by the decoherence process. We calculate the analytical probability distribution and then obtain the mixing time upper bound for small rates of decoherence. We show that it is independent of the distance parameter m and is proportional to the inverse of decoherence rate. Our paper is structured as follows: after a detailed description of the network structure LRICs in section 2, we study continuous-time quantum walks over the underlying structures in section 3. In section 4 we consider the effect of decoherence in CTQWs on LRICs and in section 5 we focus on the decoherent CTQWs when the decoherent rate is small. In section 6, we define the mixing time and obtain its upper bound. Finally, in section 7 the conclusions are presented.

2. Structure of LRICs

To construct long-range interacting cycles (LRICs), we can use the following rules. First, we construct a cycle graph of N nodes where each node is connected to its two nearest neighbor nodes. Second, all the two nodes of distance m on the cycle graph are connected by additional bonds. LRICs are denoted by $G(N, m)$ where N is the network size and m is the long-range interaction parameter. LRIC is a one-dimensional lattice with periodic boundary conditions and all nodes of the networks have four bonds [3]. The structures of $G(8, 3)$ and $G(10, 4)$ are illustrated in figure 1.

3. CTQWs on LRICs

CTQWs on LRICs are obtained by replacing the Hamiltonian of the system by the classical transfer matrix, i.e. $H = -T$ [25]. The transfer matrix T relates to the Laplace matrix by $T = -\gamma A$, where for simplicity we assume the transmission rates γ of all bonds to be equal and set $\gamma = 1$ in the following. In the Laplace matrix **A**, nondiagonal elements A_{ij} equal to 1 if nodes i and j be connected and 0 otherwise. The diagonal elements A_{ii} follow as $A_{ii} = -k_i$ that k_i is the degree of vertex i. The basis vectors $|j\rangle$ associated with the nodes j of the graph span the whole accessible Hilbert space. Then the Hamiltonian matrix H of $G(N, m)$ ($m \geqslant 2$) takes the following form:

$$H_{ij} = \langle i|H|j\rangle = \begin{cases} -4, & \text{if } i = j; \\ 1, & \text{if } i = j \pm 1; \\ 1, & \text{if } i = j \pm m; \\ 0, & \text{otherwise.} \end{cases} \tag{1}$$

The Hamiltonian acting on the state $|j\rangle$ can be written as

$$H|j\rangle = -4|j\rangle + |j-1\rangle + |j+1\rangle + |j-m\rangle + |j+m\rangle, \tag{2}$$

which is the discrete version of the Hamiltonian for a free particle moving on a lattice. It is well known in solid-state physics that the solutions of the Schrödinger equation for a particle moving freely in the regular potential are Bloch function [32, 33]. Thus, the time-independent Schrödinger equation is given by

$$\mathbf{H}|\Phi_\theta\rangle = E_\theta|\Phi_\theta\rangle, \tag{3}$$

where the eigenstates $|\Phi_\theta\rangle$ are Bloch states and can be written as a linear combination of states $|j\rangle$ localized at nodes j,

$$|\Phi_\theta\rangle = \frac{1}{\sqrt{N}} \sum_{j=1}^{N} e^{-i\theta j}|j\rangle. \tag{4}$$

The projection on the state $|j\rangle$ is $\Phi_\theta(j) = \langle j|\Phi_\theta\rangle = \frac{1}{\sqrt{N}}e^{-i\theta j}$, which is nothing but the Bloch relation $\Phi_\theta(j + 1) = e^{-i\theta}\Phi_\theta(j)$ [32, 33].

Now the energy is obtained from equations (3) and (4) as

$$E_\theta = -4 + 2\cos(\theta) + 2\cos(m\theta), \tag{5}$$

for $j = 0, 1, \ldots, N - 1$. The classical and quantum transition probabilities between two nodes can be written as

$$P_{k,j}(t) = \sum_\theta e^{-tE_\theta}\langle k|\Phi_\theta\rangle\langle\Phi_\theta|j\rangle, \tag{6}$$

$$\pi_{k,j}(t) = |\alpha_{k,j}(t)|^2 = \left|\sum_\theta e^{-itE_\theta}\langle k|\Phi_\theta\rangle\langle\Phi_\theta|j\rangle\right|^2. \tag{7}$$

4. The decoherent CTQWs on LRICs

4.1. Gurvitz's model

To analyze the decoherent continuous-time quantum walks on LRICs, we use the analytical model developed by Gurvitz [31, 34]. In this model, every node is regarded as a quantum
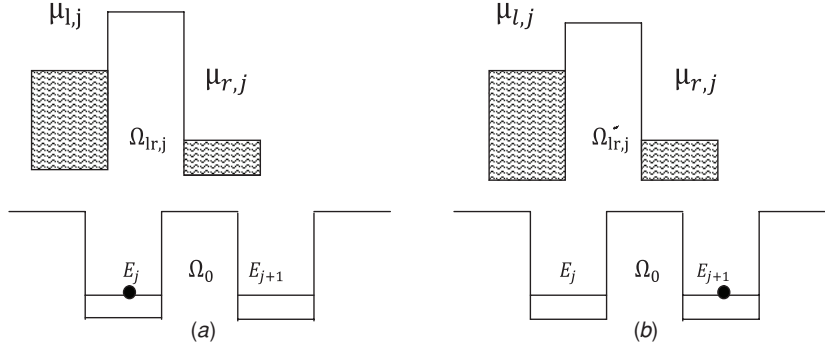
Figure 2. (*a*) Point contact detector *j* monitoring the electron in dot *j* and (*b*) point contact *j* in the presence of the electron in dot *j* + 1.

dot. Thus, LRIC is represented by a set of the identical tunnel-coupled quantum dots (QDs). The walks are done by an electron initially placed in one of dots. A ballistic point contact (PC) is placed near every dot that is taken as a noninvasive detector. We assume that all point contacts are identical. Also, they are placed far enough from quantum dots so that the tunneling between them is negligible. Moreover, for simplicity, we consider electrons as spinless fermions [30]. Each PC continuously monitors the attached quantum dot. This measurement process induces decoherence to electron walks as is shown in figure 2. Firstly, we study the simple quantum walks with the Hamiltonian [35]

$$
\begin{aligned}
H_0 &= -\sum_{ij} \Delta_{ij}(t)\big(\hat{c}_i^\dagger \hat{c}_j + \hat{c}_i \hat{c}_j^\dagger\big) + \sum_j \epsilon_j(t)\hat{c}_j^\dagger \hat{c}_j \\
&\equiv -\sum_{ij} \Delta_{ij}(t)(|i\rangle\langle j| + |j\rangle\langle i|) + \sum_j \epsilon_j(t)|j\rangle\langle j|,
\end{aligned}
\tag{8}
$$

where $|j\rangle = \hat{c}_j^\dagger|0\rangle$ denotes the state that the electron is placed at dot j. Δ_{ij} is the hopping amplitude between dots i, j and $\epsilon_j(t)$ is the on-site dot energy. We assume the constant hopping amplitude between linked dots and no on-site terms. For simplicity, we renormalize the time, so that it becomes dimensionless [36]. Hence, the Hamiltonian has the form

$$
H_0 = \frac{1}{4}\sum_{j=0}^{N-1}\big(\hat{c}_{j+1}^\dagger \hat{c}_j + \hat{c}_j^\dagger \hat{c}_{j+1} + \hat{c}_{j+m}^\dagger \hat{c}_j + \hat{c}_j^\dagger \hat{c}_{j+m}\big).
\tag{9}
$$

The tunneling Hamiltonian $H_{\mathrm{PC},j}$ describing electron transport in the point contact j can be written as [31, 36]

$$
H_{\mathrm{PC},j} = \sum_l E_{l,j}\hat{a}_{l,j}^\dagger \hat{a}_{l,j} + \sum_r E_{r,j}\hat{a}_{r,j}^\dagger \hat{a}_{r,j} + \sum_{lr}\Omega_{lr,j}\big(\hat{a}_{r,j}^\dagger \hat{a}_{l,j} + \mathrm{H.C.}\big).
\tag{10}
$$

Here, $\hat{a}_{l,j}^\dagger(\hat{a}_{l,j})$ and $\hat{a}_{r,j}^\dagger(\hat{a}_{r,j})$ are the creation (annihilation) operators in the left and right reservoirs of detector j, respectively, and $\Omega_{lr,j}$ is the hopping amplitude between the states l and r of detector j. The presence of an electron in the left dot results in an effective increase of the point-contact barrier $(\Omega_{lr} \to \Omega_{l,r} + \delta\Omega_{l,r})$, and we can represent the interaction term as [31, 36]

$$
H_{\mathrm{int},j} = \sum_{l,r}\delta\Omega_{lr,j}\hat{c}_j^\dagger \hat{c}_j\big(\hat{a}_{l,j}^\dagger \hat{a}_{r,j} + \mathrm{H.C.}\big).
\tag{11}
$$

Thus, the entire system Hamiltonian can be described by

$$H = H_0 + \sum_{j=0}^{N-1} H_{\text{PC},j} + H_{\text{int},j}. \tag{12}$$

We suppose for simplicity that the hopping amplitude of jth point contact is weakly dependent on the states l and r, so that it can be replaced by its average value, $(\Omega_{lr,j} \simeq \bar{\Omega})$ and $\delta\Omega_{lr,j} \simeq \delta\bar{\Omega}$. The occupation of the quantum dot can be measured through the variation of the detector current $\Delta I = I_2 - I_1$ where $I_1 = e2\pi\bar{\Omega}^2\rho_{l,j}\rho_{r,j}V_j$ is the detector current when the electron occupies the first dot, figure 2(a), and $I_2 = e2\pi(\bar{\Omega}^2 + \delta\bar{\Omega})^2\rho_{l,j}\rho_{r,j}V_j$ is the current flowing through the detector in the presence of the electron in the second dot, figure 2(b). The densities of states in the left and right reservoirs of detector j are $\rho_{l,j}$ and $\rho_{r,j}$ respectively and the voltage bias is the variation of the chemical potentials in the left and right reservoirs in a detector, i.e. $V_j = \mu_{l,j} - \mu_{r,j}$ [34]. Now, we are ready to write the Schrödinger equation for the entire system with Hamiltonian H. The effect of the detector on the quantum dot can be obtained by tracing out the detector states. Gurvitz has shown, for a double dot and detector together (figure 2), that the Schrödinger equation results in the evolution of a reduced density matrix traced over all states of the detector which coincides with the Bloch-type rate equations [31, 34]. These equations are as follows:

$$
\begin{aligned}
\dot{\rho}_{j,j} &= i\Omega_0(\rho_{j,j+1} - \rho_{j+1,j}), \\
\dot{\rho}_{j+1,j+1} &= i\Omega_0(\rho_{j+1,j} - \rho_{j,j+1}), \\
\dot{\rho}_{j,j+1} &= i\epsilon_j\rho_{j,j+1} + i\Omega_0(\rho_{j,j} - \rho_{j+1,j+1}) - \frac{\Gamma}{2}\rho_{j,j+1},
\end{aligned}
\tag{13}
$$

where $\epsilon_j = E_j - E_{j+1}$ and Ω_0 is the coupling between the left and right dots. Also, $\rho_{j,j+1}(t) = \rho_{j+1,j}^*(t)$ are the off-diagonal reduced density matrix elements and the diagonal terms of this density matrix $\rho_{j,j}(t)$, $\rho_{j+1,j+1}(t)$ are the probabilities of finding the electron in the jth dot and in the $(j + 1)$st dot, respectively. Moreover, $\Gamma = \left(\sqrt{\frac{I_1}{e}} - \sqrt{\frac{I_2}{e}}\right)^2\frac{V_j}{2\pi}$ is the decoherence rate due to continuous observation with a noninvasive detector [31, 34]. Applying this model to our system results in

$$
\begin{aligned}
\frac{\mathrm{d}}{\mathrm{d}t}\rho_{j,k}(t) = \frac{i}{4}[&-\rho_{j-1,k} - \rho_{j+1,k} - \rho_{j-m,k} - \rho_{j+m,k} + \rho_{j,k-1} \\
&+ \rho_{j,k+1} + \rho_{j,k-m} + \rho_{j,k+m}] - \Gamma(1 - \delta_{j,k})\rho_{j,k}.
\end{aligned}
\tag{14}
$$

Our subsequent analysis will focus on the variable $S_{j,k}$ defined as [30]

$$S_{j,k} = i^{k-j}\rho_{j,k}. \tag{15}$$

Substituting equation (15) into equation (14), we have

$$
\begin{aligned}
\frac{\mathrm{d}}{\mathrm{d}t}S_{j,k} = \frac{1}{4}[&-S_{j-1,k} + S_{j+1,k} - i^{-m+1}S_{j-m,k} - i^{m+1}S_{j+m,k} - S_{j,k-1} \\
&+ S_{j,k+1} + i^{m+1}S_{j,k-m} + i^{-m+1}S_{j,k+m}] - \Gamma(1 - \delta_{j,k})S_{j,k}.
\end{aligned}
\tag{16}
$$

5. Small decoherence

We consider the coherent continuous-time quantum walks when $\Gamma N \ll 1$. Equation (16) can be rewritten as the perturbed linear operator equation [30]

$$\frac{\mathrm{d}}{\mathrm{d}t}S(t) = (L + U)S(t), \tag{17}$$

where the linear operators L and U are

$$L^{(\mu,\nu)}_{(\alpha,\beta)} = \tfrac{1}{4}[-\delta_{\alpha,\mu+1}\delta_{\beta,\nu} + \delta_{\alpha,\mu-1}\delta_{\beta,\nu} - \mathrm{i}^{-m+1}\delta_{\alpha,\mu+m}\delta_{\beta,\nu} - \mathrm{i}^{m+1}\delta_{\alpha,\mu-m}\delta_{\beta,\nu}$$

$$- \delta_{\alpha,\mu}\delta_{\beta,\nu+1} + \delta_{\alpha,\mu}\delta_{\beta,\nu-1} + \mathrm{i}^{m+1}\delta_{\alpha,\mu}\delta_{\beta,\nu+m} + \mathrm{i}^{-m+1}\delta_{\alpha,\mu}\delta_{\beta,\nu-m}] \tag{18}$$

$$U^{(\mu,\nu)}_{(\alpha,\beta)} = -\Gamma(1 - \delta_{\alpha,\beta})\delta_{\alpha,\mu}\delta_{\beta,\nu}, \tag{19}$$

where L is an $N^2 \times N^2$ matrix and $L^{(\mu,\nu)}_{(\alpha,\beta)}$ is the entry of L indexed by the row index (μ,ν) and the column index (α,β). Also, U has the same behavior. By the above substitution, we obtain

$$\frac{\mathrm{d}}{\mathrm{d}t}S_{\alpha,\beta} = \sum_{\mu,\nu=0}^{N-1}\left(L^{(\mu,\nu)}_{(\alpha,\beta)} + U^{(\mu,\nu)}_{(\alpha,\beta)}\right)S_{\mu,\nu}, \tag{20}$$

where $0 \leqslant \alpha, \beta, \mu, \nu \leqslant N-1$. The initial conditions are

$$\rho_{\alpha,\beta}(0) = S_{\alpha,\beta}(0) = \delta_{\alpha,0}\delta_{\beta,0}. \tag{21}$$

To obtain the zero-order solution of equation (20), we require an expansion on the eigenvectors of $L^{(\mu,\nu)}_{(\alpha,\beta)}$ or

$$\sum_{\mu,\nu=0}^{N-1}L^{(\mu,\nu)}_{(\alpha,\beta)}V^{(k,l)}_{(\mu,\nu)} = \lambda^0_{(k,l)}V^{(k,l)}_{(\alpha,\beta)}, \tag{22}$$

where $0 \leqslant k, l \leqslant N-1$. After some algebra with equation (22), one can obtain

$$\lambda_{k,l} = \mathrm{i}\left[\sin\left(\frac{\pi(k+l)}{N}\right)\cos\left(\frac{\pi(k-l)}{N}\right)\right]$$

$$+ \mathrm{i}^m\left[\sin\left(\frac{\pi m(k+l)}{N}\right)\cos\left(\frac{\pi m(k-l)}{N}\right)\right] \tag{23}$$

and

$$\lambda_{k,l} = \mathrm{i}\left[\sin\left(\frac{\pi(k+l)}{N}\right)\cos\left(\frac{\pi(k-l)}{N}\right)\right]$$

$$+ \mathrm{i}^{m+1}\left[\sin\left(\frac{\pi m(k+l)}{N}\right)\sin\left(\frac{\pi m(k-l)}{N}\right)\right], \tag{24}$$

when m is an odd and even number, respectively. Eigenvectors of L are given by

$$V^{(k,l)}_{(\mu,\nu)} = \frac{1}{N}\exp\left(\frac{2\pi\mathrm{i}}{N}(k\mu + l\nu)\right). \tag{25}$$

Now, we consider eigenvalues of the unperturbed linear operator L (equations (23) and (24)) carefully. We investigate the important degeneracies of the eigenvalues $\lambda_{k,l}$ of L that lead to non-zero off-diagonal contribution of U. Firstly, due to symmetry of equation (23), we have $\lambda_{k,l} = \lambda_{l,k}$, while their eigenvectors (equation (25)) are clearly different. (Note that in equation (24) there is no such symmetry.) The second subset of degenerate eigenvalues appears when we replace $k + l \equiv 0(\mathrm{mod}N)$ in equations (23) and (24). One can see that the corresponding eigenvectors are not the same. The third subset of the degenerate eigenvalues reveals when we set $k = l$. First-order correction terms are given by the diagonal elements of equation (19) calculated on eigenvectors of equation (25). For the first subset of degenerate eigenvalues, they are equal to $-\Gamma\frac{(N-2)}{N}$. By introducing this eigenvalue perturbation to each pair of $\lambda_{(k,l)}$ with $k \neq l$ and $k + l \neq N$, the degeneracy of the first subset is removed. The degeneracy of the second subset is absent in our case since their eigenvectors are anyway excluded from the final solution by the initial condition [36]. In our discursion, there is not the degeneracy of the third subset since U is diagonal over the corresponding eigenvectors

[30]. For these eigenvalues, the correction terms are $-\Gamma\frac{(N-1)}{N}$. Thus, as mentioned in [30, 36], equation (20) can be expressed in terms of eigenvectors of equation (25):

$$S_{\alpha,\beta}(0) = \frac{\delta_{\alpha,\beta}}{N} + \frac{1}{N^2} \sum_{k,l=0}^{N-1} (1 - \delta_{k+l,0} - \delta_{k+l,N}) \exp\left[\frac{2\pi i(k\alpha + l\beta)}{N}\right]. \quad (26)$$

The full solution is of the form

$$S_{\alpha,\beta}(t) = \frac{\delta_{\alpha,\beta}}{N} + \sum_{k,l=0}^{N-1} \frac{1 - \delta_{k+l,0} - \delta_{k+l,N}}{N^2} \exp\left[\frac{2\pi i(k\alpha + l\beta)}{N}\right] e^{t(\lambda_{(k,l)} + \tilde{\lambda}_{(k,l)})}. \quad (27)$$

The probability distribution of the continuous-time quantum walks is given by the diagonal elements of the reduced density matrix $P_j(t) = S_{j,j}(t)$, that is

$$P_j(t) = \frac{1}{N} + \sum_{k,l=0}^{N-1} \frac{1 - \delta_{k+l,0} - \delta_{k+l,N}}{N^2} \exp\left[\frac{2\pi i(k+l)j}{N}\right] e^{t(\lambda_{(k,l)} + \tilde{\lambda}_{(k,l)})}. \quad (28)$$

Now, we want to rewrite the above equation for odd and even values of m, respectively.

Odd m

The solution of equation (20) is

$$P_j(t) = \frac{1}{N} + \sum_{k,l=0}^{N-1} \frac{1 - \delta_{k+l,0} - \delta_{k+l,N}}{N^2} \left[\delta_{k,l}\, e^{-\Gamma\frac{N-1}{N}t} + (1 - \delta_{k,l})\, e^{-\Gamma\frac{N-2}{N}t}\right] e^{\frac{2\pi i(k+l)j}{N}}$$

$$\times \exp\left[it \sin\left(\frac{\pi(k+l)}{N}\right) \cos\left(\frac{\pi(k-l)}{N}\right)\right.$$

$$\left. + i^m t \sin\left(\frac{\pi m(k+l)}{N}\right) \sin\left(\frac{\pi m(k-l)}{N}\right)\right]. \quad (29)$$

for odd m.

Even m

The full solution of equation (20) is

$$P_j(t) = \frac{1}{N} + \sum_{k,l=0}^{N-1} \frac{1 - \delta_{k+l,0} - \delta_{k+l,N}}{N^2} \times e^{-\Gamma\frac{N-1}{N}t} \times \exp\left[\frac{2\pi i(k+l)j}{N}\right]$$

$$\times \exp\left[it \sin\left(\frac{\pi(k+l)}{N}\right) \cos\left(\frac{\pi(k-l)}{N}\right)\right.$$

$$\left. + i^{m+1} t \sin\left(\frac{\pi m(k+l)}{N}\right) \sin\left(\frac{\pi m(k-l)}{N}\right)\right]. \quad (30)$$

for even m.

6. Mixing time

To define the mixing time of continuous-time quantum walks, we use the principal motivation to studying random walks. In computer science, the probabilistic algorithm provides the best solution for many problems. Thus, the precise solution is obtained by a well-chosen sampling distribution. Generating such a distribution is a matter of mapping the uniform distribution

into the desired one. Hence, it is important to get a truly uniform distribution [37]. The mixing time $T_{\text{mix}}(\epsilon)$ is defined as the number of steps needed before the distribution is guaranteed to be ϵ-close to the uniform distribution, or

$$T_{\text{mix}}(\epsilon) = \min \left\{ T : \sum_{j=0}^{N-1} \left| P_j(t) - \frac{1}{N} \right| \leqslant \epsilon \right\}, \tag{31}$$

where $P_j(t)$ is the probability distribution of quantum walk on the node j of the graph G and $\frac{1}{N}$ is the uniform distribution over the graph G. Based on the above analysis, we will be interested in decreasing the mixing time. Firstly, we want to calculate the upper bound on the ϵ-uniform mixing time $T_{\text{mix}}(\epsilon)$ of equation (29)(for odd m). We define

$$M_j(t) = \frac{1}{N} \sum_{k=0}^{N-1} \exp \left[\mathrm{i}t \sin \left(\frac{2\pi k}{N} \right) + \mathrm{i}^m t \sin \left(\frac{2\pi km}{N} \right) \right] \mathrm{e}^{\frac{2\pi \mathrm{i}kj}{N}}. \tag{32}$$

Hence, we have

$$M_j^2 \left(\frac{t}{2} \right) = \frac{1}{N^2} \sum_{k,l=0}^{N-1} \mathrm{e}^{t\lambda_{(k,l)}} \mathrm{e}^{\frac{2\pi \mathrm{i}(k+l)j}{N}}, \qquad M_{2j}(t) = \frac{1}{N} \sum_{k=0}^{N-1} \mathrm{e}^{t\lambda_{(k,k)}} \mathrm{e}^{\frac{2\pi \mathrm{i}k(2j)}{N}}.$$

Hence, equation (29) can be rewritten as

$$\left| P_j(t) - \frac{1}{N} \right| = \mathrm{e}^{-\Gamma \frac{N-2}{N} t} \left| M_j^2 \left(\frac{t}{2} \right) - \frac{1}{N} + \frac{\mathrm{e}^{-\frac{\Gamma t}{N}} - 1}{N} \left[M_{2j}(t) - \frac{2 - N \bmod 2}{N} \right] \right|. \tag{33}$$

Since $|M_j(t)| \leqslant 1$, we obtain

$$\left| P_j(t) - \frac{1}{N} \right| \leqslant \mathrm{e}^{-\Gamma \frac{N-2}{N} t} \left| 1 - \frac{1}{N} + \frac{\mathrm{e}^{-\frac{\Gamma t}{N}} - 1}{N} \left[1 - \frac{2 - N \bmod 2}{N} \right] \right|,$$

$$\leqslant \mathrm{e}^{-\Gamma \frac{N-2}{N} t} \left| 1 + \frac{\mathrm{e}^{-\frac{\Gamma t}{N}} - 1}{N} \left(1 - \frac{2}{N} \right) \right|. \tag{34}$$

Based on the definition of time mixing,

$$\sum_{j=0}^{N-1} \left| P_j(t) - \frac{1}{N} \right| \leqslant \mathrm{e}^{-\Gamma \frac{N-2}{N} t} (N + \mathrm{e}^{\frac{-t\Gamma}{N}} - 1). \tag{35}$$

Because of $\mathrm{e}^{-\frac{\Gamma t}{N}} \leqslant 1$, the above equation reduces to $N \mathrm{e}^{-\Gamma \frac{N-2}{N} t} \leqslant \epsilon$. As a result, we obtain the mixing time upper bound of

$$T_{\text{mix}}(\epsilon) < \frac{1}{\Gamma} \ln \left(\frac{N}{\epsilon} \right) \left[1 + \frac{2}{N-2} \right]. \tag{36}$$

This relation is in agreement with the result that is mentioned in [30] for the cycle. Note that in this case, the mixing time lower bound cannot derive equation (33) easily, since there is a relation between $M_j^2(\frac{t}{2})$ and $M_{2j}(t)$. Now, we calculate the upper bound on $T_{\text{mix}}(\epsilon)$ of equation (30)(for even m). We define

$$M_j(t) = \frac{1}{N^2} \sum_{k,l=0}^{N-1} \exp \left[\mathrm{i} \frac{t}{2} \left(\sin \left(\frac{2\pi k}{N} \right) + \sin \left(\frac{2\pi l}{N} \right) \right) \right] \mathrm{e}^{\frac{2\pi \mathrm{i}(k+l)j}{N}}$$

$$\times \exp \left[-\mathrm{i}^{m+1} \frac{t}{2} \left(\cos \left(\frac{2\pi km}{N} \right) - \cos \left(\frac{2\pi lm}{N} \right) \right) \right]. \tag{37}$$

Thus, we have

$$\left| P_j(t) - \frac{1}{N} \right| = e^{-\Gamma \frac{N-1}{N}t} \left| M_j(t) - \frac{1}{N} \right|$$

$$\leqslant e^{-\Gamma \frac{N-1}{N}t} \left[1 + \frac{1}{N} \right] \tag{38}$$

and with summation over j and using the mixing time definition, we get $N e^{-\Gamma \frac{N-1}{N}t} \leqslant \epsilon$. This gives the mixing time upper bound of

$$T_{\text{mix}}(\epsilon) \leqslant \frac{1}{\Gamma} \left[1 + \frac{1}{N-1} \right] \ln\left(\frac{N}{\epsilon} \right). \tag{39}$$

The lower bound of mixing time can be derived by the first equality of equation (38) as

$$\left| P_j(t) - \frac{1}{N} \right| = e^{-\Gamma \frac{N-1}{N}t} \left| M_j(t) - \frac{1}{N} \right|$$

$$= 0 \tag{40}$$

where in the last inequality, we set $M_j(t) = \frac{1}{N}$. In other words, in this time the quantum walk completely reaches the uniform distribution $\frac{1}{N}$.

Thus, the lower bound of mixing time follows as

$$T_{\text{mix}}(\epsilon) \geqslant 0. \tag{41}$$

Equations (36) and (39) show that the T_{mix} upper bound is independent of the distance parameter m. Moreover, since we approximated the coefficient of the exponential function in equations (34) and (38), the mixing time upper bound is exactly proportional to $\frac{1}{\Gamma}$ that accord with Fedichkin, Solenov and Tamon's result for the continuous-time quantum walks on cycles [30]. Also, these relations prove that the mixing time upper bound for even m is smaller than the mixing time upper bound for odd m.

7. Conclusion

We have studied continuous-time quantum walks on long-range interacting cycles (LRICs) under small decoherence $\Gamma N \ll 1$. We obtained the probability distribution analytically and found that the mixing time upper bound for odd values of m ($T_{\text{mix}}(\epsilon) < \frac{1}{\Gamma} \ln(\frac{N}{\epsilon})[\frac{N}{N-2}]$) is larger than the mixing time upper bound for even m ($T_{\text{mix}}(\epsilon) \leqslant \frac{1}{\Gamma} \ln(\frac{N}{\epsilon})[\frac{N}{N-1}]$). These relations show that the T_{mix} upper bound is inversely proportional to the decoherence rate Γ and is independent of the distance parameter m. Also, we proved that for even m the lower bound time mixing is zero. In other words, we have shown that $T_{\text{mix}}(\epsilon)$ decrease with Γ at least as fast as $1/\Gamma$.

References

[1] Aharonov D, Ambainis A, Kempe J and Vazirani U 2001 *Proc. of ACM Symp. on Theory of Computation (STOC 01)*
[2] Kim B J, Hong H and Choi M Y 2003 *Phys. Rev.* B **68** 014304
[3] Xu X 2009 *Phys. Rev.* E **79** 011117
[4] Wójcik D K and Dorfman J R 2003 *Phys. Rev. Lett.* **90** 230602
[5] Meyer D A 1996 *J. Stat. Phys.* **85** 551
[6] Burn T A, Carteret H A and Ambainis A 2003 *Phys. Rev. Lett.* **91** 130602
[7] Ahmadi A, Belk R, Tamon C and Wendler C 2003 *Quantum Inf. Comput.* **3** 611–8
[8] Chisaki K, Hamada M, Konno N and Segawa E 2009 arXiv:quant-ph/0903.4047

  [9] Konno N 2009 *Quantum Inf. Process.* **8** 387
 [10] Chadrashekar C M 2006 arXiv:quant-ph/0609113
 [11] Chandrashekar C M, Srikanth R and Laflamme R 2008 *Phys. Rev.* A **77** 032326
 [12] Gottlieb A D 2004 *Phys. Rev.* E **72** 047102
 [13] Moore C and Russell A 2002 Quantum Walks on the Hypercube *Proc. of the 6th Workshop on Randomization and Approximation Techniques in Computer Science* (*Lecture Notes in Computer Science* vol 2483) ed J D P Rolim and S Vadhan (Berlin: Springer) pp 164–78
 [14] Salimi S 2009 *Ann. Phys.* **324** 1185
 [15] Xu X-P 2009 *J. Phys. A: Math. Theor.* **42** 115205
 [16] Mulken O, Pernice V and Blumen A 2007 *Phys. Rev.* E **76** 051125
 [17] Salimi S 2008 *Int. J. Quantum Inf.* **6** 945
 [18] Jafarizadeh M A and Salimi S 2007 *Ann. Phys.* **322** 1005
 [19] Jafarizadeh M A, Sufiani R, Salimi S and Jafarizadeh S 2007 *Eur. Phys. J.* B **59** 199
 [20] Konno N 2005 *Phy. Rev.* E **72** 026113
 [21] Mulken O, Bierbaum V and Blumen A 2006 *J. Chem. Phys.* **124** 124905
 [22] Jafarizadeh M A and Salimi S 2006 *J. Phys. A: Math. Gen.* **39** 13295
 [23] Lo P, Rajaram S, Schepens D, Sullivan D, Tamon C and Ward J 2006 *Quantum Inf. Comput.* **6** 370
 [24] Salimi S 2008 *Int. J. Theor. Phys.* **47** 3298
 [25] Farhi E and Gutmann S 1998 *Phys. Rev.* A **58** 915
 [26] Konno N 2006 Infinite dimensional analysis *Quantum Probab. Relat. Top.* **9** 287
 [27] Kendon V and Tregenna B 2003 *Phy. Rev.* A **67** 042315
 [28] Romanelli A, Siri R, Abal G, Auyuanet A and Donangelo R 2005 *Phys. Rev.* A **347G** 137-52
 [29] Strauch W 2009 arXiv:quanth-ph/0808.3403
 [30] Fedichkin L, Solenov D and Tamon C 2006 *Quantum Inf. Comput.* **6** 263
 [31] Gurvitz A 1997 *Phy. Rev.* B **56** 15215
 [32] Ziman J M 1972 *Principles of the Theory of Solids* (Cambridge: Cambridge University Press)
 [33] Kittel C 1986 *Introduction to Solid State Physics* (New York: Wiley)
 [34] Gurvitz A, Fedichkin L, Mozyrsky D and Berman P 2003 *Phy. Rev. lett.* **91** 066801
 [35] Hines A P and Stamp P C E 2007 arXiv:quant-ph/0701088
 [36] Solenov D and Fedichkin L 2006 *Phys. Rev.* A **73** 012313
 [37] Drezgic M, Hines A P, Sarovar M and Sastry S 2008 arXiv:quant-ph/0811.4472